Desalination and Water Treatment
www.deswater.com

doi: 10.5004/dwt.2019.23936

155 (2019) 84–93
July

Adsorption kinetic, equilibrium and thermodynamic studies of Eosin-B onto anion exchange membrane

Muhammad Imran Khan[a,b,*], Mushtaq Hussain Lashari[c], Majeda Khraisheh[d], Shabnam Shahida[e], Shagufta Zafar[f], Prasert Prapamonthon[g], Aziz ur Rehman[h], Saima Anjum[f], Naseem Akhtar[f], Farzana Hanif[f]

[a]*School of Chemistry and Material Science, University of Science and Technology of China, Hefei 230026, Anhui, China, email: raoimranishaq@gmail.com (M.I. Khan)*
[b]*Fujian Institute of Research on the Structure of Matter, Chinese Academy of Sciences, Fuzhou 350002, Fujian, China*
[c]*Department of Zoology, The Islamia University of Bahawalpur, Bahawalpur 63100, Pakistan, email: mushtaqlashary@gmail.com*
[d]*Department of Chemical Engineering, College of Engineering, Qatar University, Doha, Qatar, email: m.khraisheh@qu.edu.qa*
[e]*Department of Chemistry, The University of Poonch, Rawalakot, Azad Jammu & Kashmir, Pakistan, email: shabnamshahida01@gmail.com*
[f]*Department of Chemistry, The Government Sadiq College Women University, Bahawalpur 63000, Pakistan, emails: shg_zf@yahoo.com (S. Zafar), drsaima@gscwu.edu.pk (S. Anjum), drnaseem@gscwu.edu.pk (N. Akhtar), farzanakhan@yahoo.com (F. Hanif)*
[g]*King Mongkut's Institute of Technology Ladkrabang, Bangkok, Thailand, email: prasert.pr@kmitl.ac.th*
[h]*Department of Chemistry, The Islamia University of Bahawalpur, Bahawalpur 63100, Pakistan, email: azizypk@yahoo.com*

Received 8 September 2018; Accepted 9 February 2019

ABSTRACT

In this research, batch adsorption of anionic dye Eosin-B (EB) onto anion exchange membrane (AEM) (BI) from aqueous solution has been investigated at room temperature. The effect of some operating conditions such as contact time, membrane dosage, initial dye concentration and temperature on the percentage removal of EB from aqueous solution has been investigated in detail. Moreover, adsorption kinetics has been analyzed using different models such as pseudo-first-order, pseudo-second-order, Elovich, liquid film diffusion, modified Freundlich and Bangham models. Results show that adsorption data fits to the pseudo-second order kinetics very well. Non-linear isotherms containing two parameters and three parameters isotherms have been applied on experimental data. Different thermodynamic parameters such as Gibb's free energy ($\Delta G°$), enthalpy ($\Delta H°$), and entropy ($\Delta S°$) have been calculated, which shows that adsorption of EB onto anion exchange membrane (B1) is an exothermic process.

Keywords: Adsorption; Anion exchange membranes; Eosin-B; Kinetics; Isotherm; Thermodynamics

1. Introduction

One of the most pervasive environmental problem afflicting people throughout the world is water pollution and inadequate access to clean water. One of the dangerous pollutants in water is synthetic dyes containing some components or moieties that could be toxic, carcinogenic, and teratogenic or mutangenic or aquatic life and humans. Synthetic dyes are used extensively in textile, paper, food, rubber and printing industries. Worldwide, approximately 10%–15% of

* Corresponding author.

the total dyes used in various textile processes and in other industries are discharged into wastewater causing extensive pollution [1]. There is an extremely requirement for the removal of dyes from wastewater.

Ion-exchange membranes (IEMs) are one of the main technologies available in different energy and separation processes. Recently, commercial anion exchange membranes (AEMs) have been exposed to have notable adsorption capacities. The macro porous membrane systems have ability to remove the technical limitations of packed-bed operations. Moreover, it can improve the potential of the membrane to scale-up. Accordingly IEMs are developed as a potentially substitute adsorbent for industrial applications. Nowadays researchers try to find different cost effective sustainable substitute to commercial activated carbon adsorbents. Numerous review articles in the removal of dyes from aqueous solution are available [2–4]. Nevertheless, more fundamental studies are needed to understand adsorption mechanisms such as kinetics, and thermodynamics in a better way.

Among several chemical, physical and biological technologies, adsorption is one of the effective methods to remove dyes from wastewater. Adsorption is known to be a better technique which has great importance due to the ease of operations and comparable low cost of applications in decoloration process [5]. This provides an attractive alternative for the treatment of contaminated water, especially if the sorbent is inexpensive and does not require an additional pretreatment step before its applications [6].

Activated carbon is one of the commonly used adsorbent which has a high removal capacity for the dye/organics [7–9]. However, some of its disadvantages are the high cost of the treatment and its difficulty to regenerate the adsorbent which increase the cost of wastewater treatment more. Therefore, there is demand for other adsorbents which are made up of inexpensive material and locally available such that adsorption process will become economically viable. Investigators have studied the feasibility of using low cost adsorbents such as waste apricot [10], coconut shells [11], dairy sludge [12], bamboo grass treated with concentrated sulfuric acid, peat [13], orange peels [14], peanut hulls [15], rice husk [16], ground nut shell charcoal and bagasse [17], bamboo [18], jack fruit peels [19], pistachio nut shell [20], date stone, and palm tree waste [21] as adsorbent for removal of dyes and heavy metals from wastewater. Their cost and efficiency varied from one adsorbent to another.

Presently, almost all the adsorbents developed for removal of heavy metal ions and dyes rely on the interaction of the target compounds with the functional groups that are present on the surfaces of the adsorbents [22]. Therefore, a large surface area and several adsorption sites of the matrix are necessary for adsorption affinity of membranes to remove the contaminants from wastewater, and the specific surface area was one of the most significant parameter to influence the adsorption capacity of the adsorbents [23–25]. Thus, the AEM become a good choice as adsorbent for dye removal from aqueous solution because it exhibits large surface area for adsorption. Cationic dye methyl violet 2B was removed from aqueous solution by two kinds of membranes P81 and ICE450 via adsorption process [26]. Similarly, AEMs was developed for adsorption removal of anionic dye Cibacron Blue 3GA from aqueous solution [27]. In our previous research, we have employed AEMs for removal of different dyes from water via adsorption process [28–31]. In order to extend it, we report the use of a new AEM (BI) as an adsorbent for removal of EB from aqueous solution at room temperature. The purpose of this work is to study the removal of anionic dye EB by adsorption onto BI from aqueous solution. The effect of contact time, mass of adsorbent, initial dye concentration and temperature has been analyzed in detail. Adsorption kinetic, equilibrium and thermodynamic endowments have been revealed to explain the rate and mechanism of adsorption to determine the factor which controls the rate of adsorption and to find out the possibility of employing these adsorbents (anion exchange membrane BI) as a good adsorbent for removal of EB from aqueous solution at room temperature.

2. Experimental, materials and procedures

2.1. Adsorbent

The commercial AEM BI provided by Chemjoy Membrane Co. Ltd, Hefei, Anhui, China was used as an adsorbent. It was prepared from blends of polyvinyl alcohol (PVA) and quaternized poly (2, 6-dimethyl-1,4-phenylene oxide) (QPPO) [29]. It was used without further treatment. The ion exchange capacity (IEC) and water uptake (W_R) of BI are 0.55 mmol g^{-1} and 42.7% respectively [29].

2.2. Adsorbate

The commercial anionic dye Eosin-B (EB), obtained from Fluka chemicals was used as adsorbate. A stock solution of 1,000 mg L^{-1} was prepared by dissolving 1.0 g of accurately weighed EB into 1 L of deionized water and required concentrations were obtained by further dilution of stock solution. All the chemicals used in the experiments were of analytical grade. The structures of EB are shown in Fig. 1.

2.3. Adsorption experiment

Adsorption measurements were carried out by batch mode as reported in our previous work [28,31,32]. In a typical

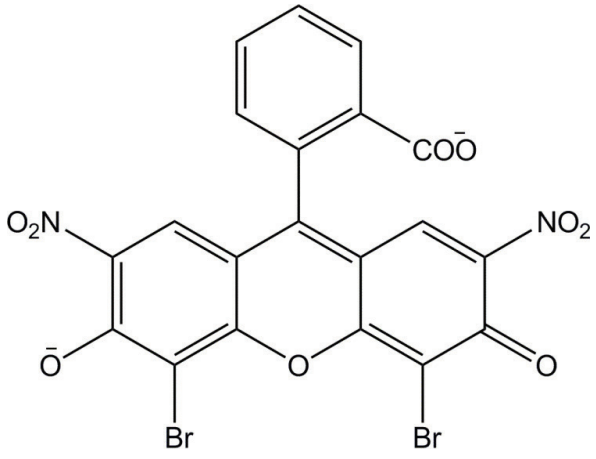

Fig. 1. Chemical strucure of Eosin-B (EB) dye.

experiment, batch adsorption of EB was done by immersing known amount of adsorbent (BI) into 40 ml of dye aqueous solutions of known concentration at room temperature. The flasks were shaked at a constant speed of 120 rpm. At predetermined time, the flasks were withdrawn from the shaker and residual dye concentration in the reaction mixture was determined by measuring the absorbance of the supernatant by UV/VIS spectrophotometer (UV-2550, SHIMADZU) at the wavelength (λ_{max}.= 464 nm for Eosin-B) that corresponds to the maximum absorbance of the sample. Dye concentration in the reaction mixture was calculated from the calibration curve. Adsorption experiments were conducted by varying contact time, membrane dose, initial dye concentration and temperature under the aspect of adsorption kinetics, isotherm and thermodynamic study. The EB adsorption onto BI at time t, was calculated by Eq. (1):

$$q_t = \frac{C_o - C_t}{W} \times V \quad (1)$$

where C_o and C_t are the concentration of EB at initial state and at time t respectively. Similarly V and W are volume of EB aqueous solution and weight of adsorbent respectively.

3. Results and discussion

3.1. Effect of operational parameters

In this section, the effect of operational parameters such as contact time, membrane dosage, initial concentration dye solution and temperature on the percentage removal of EB from aqueous solution have been studied. Their details are given below.

3.1.1. Effect of contact time

Fig. 2 represents the percentage removal of EB from aqueous solution as a function of contact time at room temperature. This was studied under constant conditions such as initial dye concentration, mass of adsorbent, shaking speed, volume of dye solution and temperature. It can be observed that the removal of EB was increased with contact time. The removal of dye was fast at start and then slowed down and continued to increase until equilibrium is achieved. It is because of presence of several adsorption sites onto membrane surface in the initial stage of reaction, which slowly gets saturated with the dye at increasing contact times. Repulsive forces between solute molecules on the solid and bulk phase can also contribute to the observed moderate rates of adsorption after the first 2–3 h [28].

3.1.2. Effect of membrane dosage

The effect of mass of adsorbent (anion exchange membrane BI) on the removal of dye from aqueous solution was investigated at constant conditions of contact time, adsorbent dose, initial dye concentration, volume of dye solution, shaking speed and temperature. The attained results are illustrated in Fig. 3. The removal of dye from aqueous solution is found to be increased with increasing the mass of adsorbent which is attributed to the increase in the number of available sorption sites on the surface of anion exchange membrane (BI). The removal of dye from aqueous solution was rapid at start and remains unchanged with increase in the mass of adsorbent as shown in Fig. 3. It can be seen from the attained results that EB was almost completely removed from aqueous solution at 0.1 g mass of membrane. Therefore, the mass of membrane 0.1 g was selected as optimum quantity and used in further experiments. The observed two stage-dependent adsorption behavior has also been previously reported in the literature [28].

3.1.3. Effect of initial dye concentration

The effect of initial dye concentration on the percentage removal of EB from aqueous solution was investigated keeping contact time, mass of adsorbent, volume of dye solution and shaking speed constant and attained resulted are illustrated in Fig. 4. The removal of EB is found to be decreased with increase in the initial dye concentration of solution. This is associated to the increase in EB concentration, surface area and active sites of AEMs were saturated and therefore the removal of EB from aqueous solution was decrease.

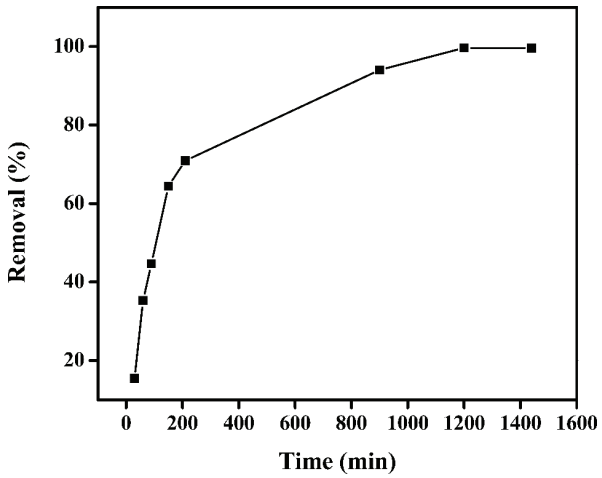

Fig. 2. Effect of contact time onto adsorption of EB onto BI.

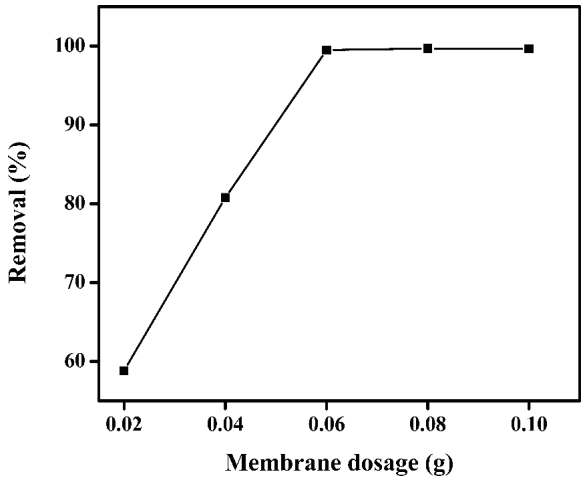

Fig. 3. Effect of membrane dosage onto adsorption of EB onto BI.

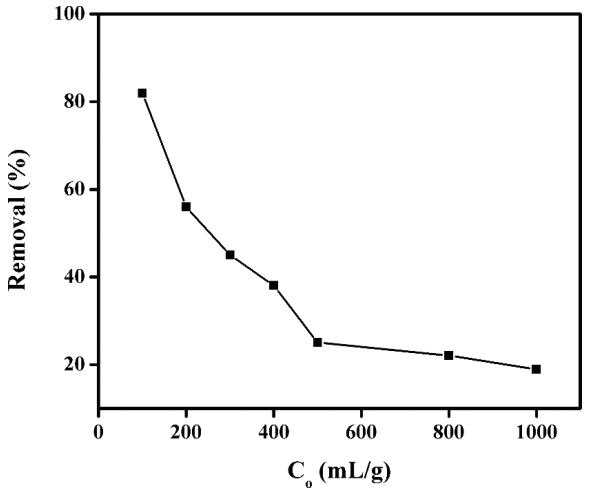

Fig. 4. Effect of initial dye concentration on the adsorption of EB onto BI.

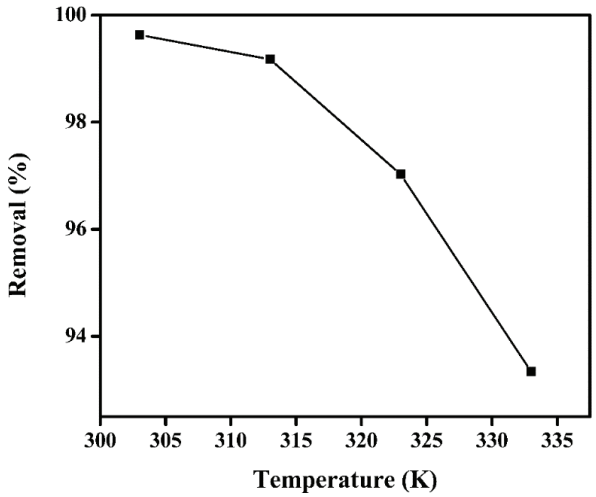

Fig. 5. Effect of temperature onto adsorption of EB onto BI.

3.1.4. Effect of temperature

Fig. 5 illustrates the effect of temperature on the percentage removal of EB from aqueous solution. It was investigated under the constant conditions of operating parameters on the system such as contact time, mass of membrane, initial dye concentration, volume of dye solution and shaking speed. It can be seen that the percentage removal of EB from aqueous was found to be decreased with increase in the temperature. It is associated to the decrease in surface activity with increasing temperature [30,33]. Therefore, the adsorption of anionic dye EB onto BI is an exothermic process.

3.2. Adsorption kinetics

3.2.1. Pseudo-first-order model

The linearized form of the Lagergren Pseudo-first-order rate equation is given by [34].

$$\log(q_e - q_t) = \log q_e - \frac{K_1 t}{2.303} \quad (2)$$

where q_e and q_t are amounts of dye adsorbed at equilibrium and time t repectively and k_1 (min^{-1}) is the rate constant of pseudo-first-order adsorption model. The plot of log(q_e–q_t) vs. time for pseudo-first-order model is depicted in Fig. 6. The value K_1 is calculated from slope of plot and given in Table 1. This plot is linear but coefficient of regression is low so the linearity of this curve does not necessarily assure the mechanism due to the inherent disadvantage of correctly estimating equilibrium adsorption capacity. There is a large difference between experimental adsorption capacity value ($q_{e,\exp}$) (19.78 mg g^{-1}) and calculated adsorption capacity value ($q_{e,\text{cal}}$) (13.78 mg g^{-1}), therefore pseudo-first-order model does not explain the rate process.

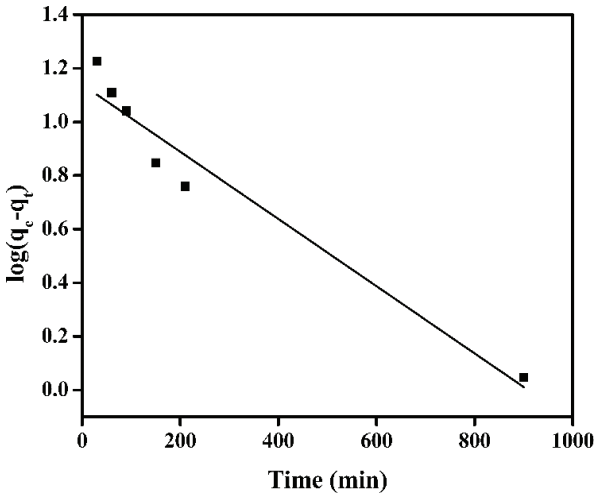

Fig. 6. Pseudo-first-order kinetics for adsorption of EB onto BI.

Table 1
Pseudo-first-order, pseudo-second-order and Elovich model rate constants (q_e = mg g^{-1}; k_1 = min^{-1}; k_2 = g mg.min^{-1}; α = mg g.min^{-1}; β = g mg^{-1})

Pseudo-first order		Pseudo-second order		Elovich model	
$q_{e,\exp}$	19.93	q_e	21.93	α	0.23
$q_{e,\text{cal}}$	13.78	$k_2 \times 10^{-4}$	3.40	β	0.23(2)
$k_1 \times 10^{-3}$	1.25	–	–	–	–
R^2	0.939	R^2	0.998	R^2	0.968

3.2.2. Pseudo-second-order model

The linearized form of pseudo-second kinetic model is expressed as [33]:

$$\frac{t}{q_t} = \frac{1}{k_2 q_e^2} + \frac{t}{q_e} \quad (3)$$

where k_2 (g mg.min^{-1}) is the rate constant of pseudo-second-order model. The graphical representation of pseudo-second-order model is shown in Fig. 7. The values of adsorption capacity (q_e) and rate constants can be determined

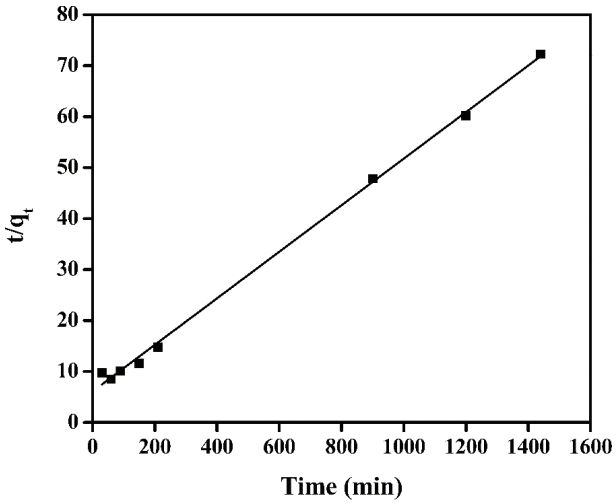

Fig. 7. Pseudo-second-order kinetics for adsorption of EB onto BI.

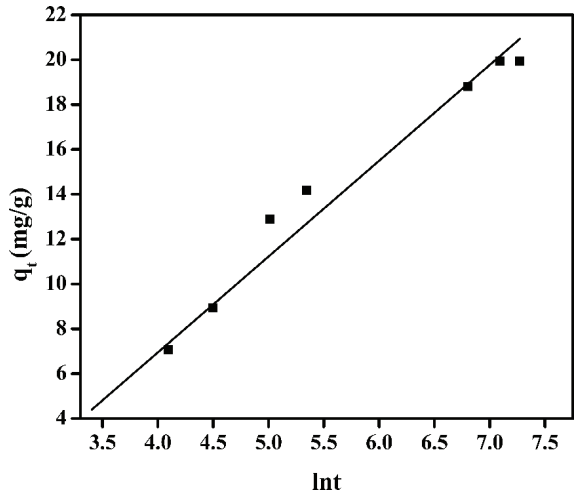

Fig. 8. Elovich model for adsorption of EB onto BI.

from slope and intercept of linear plot and are given in Table 1. The numerical values of experimental adsorption capacity ($q_{e,exp}$) (19.93 mg g^{-1}) and calculated adsorption capacity ($q_{e,cal}$) (21.93 mg g^{-1}) are very close. Moreover, the correlation coefficient ($R^2 > 0.99$) is close to unity which exhibits that adorption data fitted well to the pseudo-second-order model.

3.2.3. Elovich model

The Elovich kinetic model is an interesting model to describe the activated chemisorption for any adsorption system and it can be expressed as [35]:

$$q_t = \frac{1}{\beta}\ln(\alpha\beta) + \frac{1}{\beta}\ln t \tag{4}$$

where α and β are Elovich constants and α is considered as initial sorption rate (mg g.min^{-1}) and β is related to the extent of surface coverage and activation energy for the chemisorption. The plot of q_t vs. ln$t$ for Elovich model is given in Fig. 8. The values of α and β were determined from intercept and slope of linear plot of q_t vs. ln$t$ and are given in Table 1. The value of correlation coefficient (R^2) was 0.968 lower than that of pseudo-second-order model.

3.2.4. Liquid film diffusion model

The liquid film model is expressed as [36]:

$$\mathrm{Ln}(1-F) = -K_{fd}t \tag{5}$$

where K_{fd} is liquid film diffusion rate constant, and $F = q_t/q$. The plot of ln(1–F) vs. time for liquid film model is given in Fig. 9. The value of K_{fd} was calculated from slope of plot and is given in Table 2. The value of correlation coefficient (R^2) was 0.939 lower than pseudo-second-order model which indicates that liquid film diffusion model is not suitable to explain the experimental data for adsorption of EB onto membrane BI.

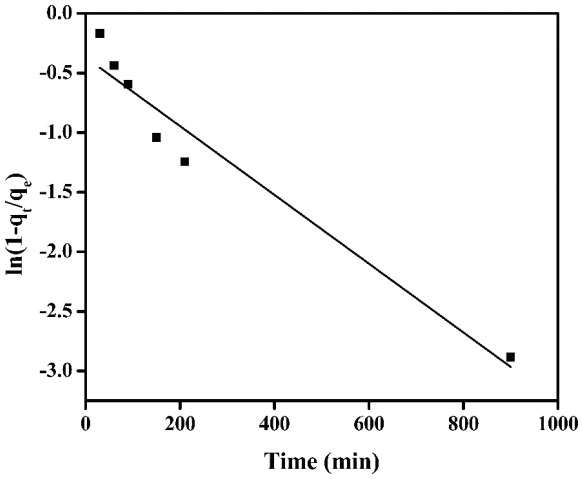

Fig. 9. Liquid film diffusion model for adsorption of EB onto BI.

Table 2
Liquid film diffusion model, modified Freundlich equation and Bangham equation rate constant (k_{fd} = min^{-1}; k = L g.min^{-1}; k_o = mL g^{-1} L^{-1})

Liquid film diffusion model		Modified Freundlich equation		Bangham equation	
$k_{fd} \times 10^{-3}$	2.89	m	2.44	k_o	0.98
C_{fd}	–0.37	k	0.025	α	0.41
R^2	0.939	R^2	0.819	R^2	0.821

3.2.5. Modified Freundlich equation

The modified freundlich eaquation was originally developed by Kuo and Lotse [37].

$$q_t = kC_o t^{1/m} \tag{6}$$

where q_t is amount of adsorbed dye (mg g^{-1}) at time t, k is apparent adsorption rate constant (L g.min^{-1}), C_o is the initial

dye concentration (mg L^{-1}), t is the contact time (min) and m is the Kuo-Lotse constant. The values of k and m were used to evaluate the effect of dye surface loading and ionic strength on the adsorption process.

Linear form of modified Freundlich equation is given as:

$$\ln q_t = \ln\left(kC_o\right) + \frac{1}{m}\ln t \tag{7}$$

The graphical representation of modified Freundlich model is given in Fig. 10. The parameters m and k were determined from slope and intercept and are given in Table 2. The correlation coefficient values was 0.819.

3.2.6. Bangham equation

Bangham equation is given as [38]:

$$\log\left(\frac{C_o}{C_o - q_t m}\right) = \log\left(\frac{k_o m}{2.303V}\right) + \alpha \log t \tag{8}$$

where C_o is the initial dye concentration (mg L^{-1}), V is volume of solution (mL), q_t is the amount of dye adsorbed (mg g^{-1}) at time t, m is the weight of adsorbent used (g L^{-1}). α and k_o (mL/g/L) are the constants of Bangham equation. The plot of $\log(C_o/C_o\text{-}q_t m)$ vs. log$t$ is the straight line with correlation coefficient 0.821 and is given in Fig. 11. The values of α and k_o were calculated from slope and intercept and are given in Table 2. The double logarithmic plot did not give linear curves for EB removal by BI indicating that the diffusion of dye into pores of the membrane is not the only rate controlling step [30]. It can be concluded that both film and pore diffusion were crucial to different extent in the removal EB from aqueous solution.

3.3. Adsorption isotherms

Adsorption isotherms are important as many informations can be depicted from them such as adsoprtion capacity and interactions between adsorbent and adsorbate. The adsorption isotherms are drawn between the quantity of dye adsorbed per gram of membranes "Q_e" and the quantity of dye left in equilibrium solution C_e and is shown in Fig. 12. The adsorption isotherm shows that adsorption capacity "Q_e" increases with the dye concentration and the distribution of dye between solid and liquid phases at equilibrium state. Most suitbale adsorption isotherm can be find out by the analysis of experimental data to different isotherm models that can be used to describe the adsorption process [39].

Several isotherm models were developed to describe the isotherm data. Two paramters isotherms include Langmuir, Freundlich, Temkin and Dubinin-Radushkevich (D-R) whereas three parameters isotherm models are Redlich-Peterson, Hill and SIPS which were used to reveal the experimental data of EB adsorption onto BI. Nonlinear methodid preferred for adsorption isotherm parameters determination over linear method. In linear method it is assumed that the scattered points around the line follow a Gaussian distribution and that the distribution error is the same at every value

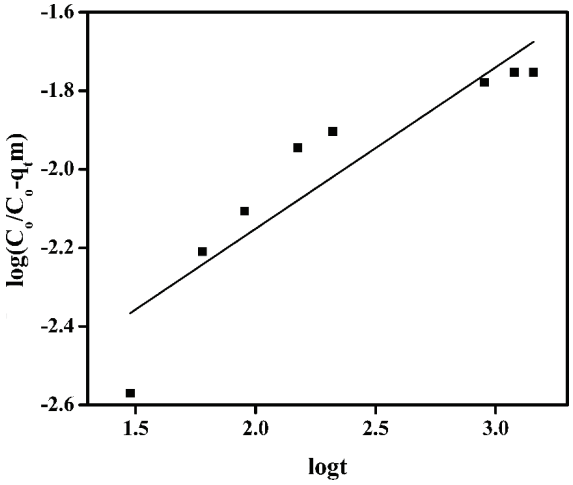

Fig. 11. Bangham equation plot between log$t$ vs $\log(C_o/C_o - mq_t)$ for adsorption of EB onto BI.

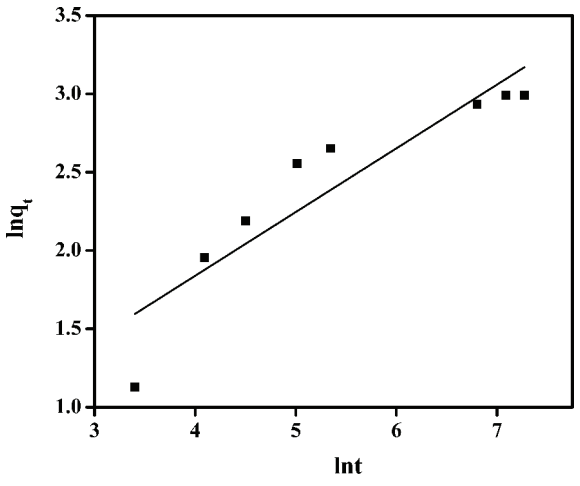

Fig. 10. Modified Freundlich equation plot between ln$t$ vs. lnq_t for adsorption of EB onto BI.

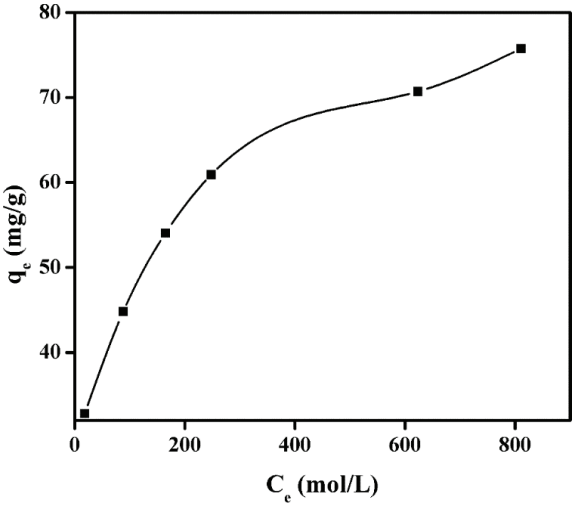

Fig. 12. Adsorption isotherm for adsorption of EB onto BI.

of the abscissa which is virtually impossible with equilibrium isotherm models, as most of the isotherm models are nonlinear. Thus, the error distribution will alter after transforming the data into a linear form [40,41]. All the model parameters were evaluated by non-linear regression using Igor Pro. WaveMatrices 6.2.1 software [42]. The nonlinear chi-square test (χ^2) is a statistical tool required for the best fit of an adsorption data and its small value indicates similarities of the experimental data while large value shows variation of experimental data [43].

3.3.1. Two parameters adsorption isotherms

Freundlich, Langmuir, Dubinin-Radushkevich (D-R) and Temkin isotherms are two parameters isotherms models which were applied in these studies.

Freundlich model is an empirical isotherm model used to explain the heterogeneous system. Nonlinear form of Freundlich isotherm model is expressed as [44]:

$$q_e = K_f C_e^{1/n} \tag{9}$$

where C_e is the supernatant concentration at equilibrium state of the system (mol L^{-1}), and q_e is the amount of dye adsorbed at equilibrium state of system (mol g^{-1}), K_f and n are Freundlich parameters. The values of K_f and n are calculated from nonlinear plot of Freundlich isotherms and are given in Table 3. The chi-square test (χ^2) is 5.58×10^{-8} showing that the experimtal data followed the Freundlich istherm model. The value of Freundlich contant n decides the favourability of adsorption process whereas K_f is the adsorption capacity of the adsorbent.

Table 3
Adsorption isotherm parameters of EB adsorption onto BI by nonlinear method

Two parameters isotherms				
Freundlich	K_f	n		5.85×10^{-8}
	3,295	0.569		
Langmuir	Q_m	K_L		1.36×10^{-7}
	3.71×10^{-3}	942.98		
D-R	C_m	β		7.48×10^{-8}
	517.6	7.32×10^{-3}		
	E = 9.604 kJmol^{-1}			
Temkin	a_T	b_T		5.96×10^{-8}
	16,281	3.67×10^{6}		
Three parameters isotherms				
Redlich-Peterson	K_{RP}	a_{RP}	g	1.85×10^{-8}
	17.097	326.36	1.304	
Hill	q_h	n_h	K_h	5.41×10^{-8}
	47.02	1.823	0.00766	
SIPS	a_s	beta	K_s	4.69×10^{-9}
	4,754	0.965	0.543	

Langmuir adsorption isotherm depends upon the maximum adsorption coincides to the saturated monolayer of liquid (adsorbate) molecules on the solid (adsorbent) surface. The nonlinear form of Langmuir model is given as follows [45]:

$$q_e = \frac{Q_m k_L C_e}{1 + k_L C_e} \tag{10}$$

where K_L is Langmuir constant (L mol^{-1}) and Q_m is Langmuir monolayer adsorption capacity (mol g^{-1}). The nonlinear plot of Langmuir model is shown in Fig. 13. The values of Q_m and K_L are given in Table 3. The chi-square test (χ^2) value was very small indicating that the adsorption of EB onto BI fitted well to the Langmuir model.

Dubinin-Redushkevich (D-R) model was used to distinguish between physical and chemical adsorption for the adsorpion of EB onto BI membrane [46]. The nonlinear D-R model is expressed as:

$$q_e = C_m \exp\left(-\beta\varepsilon^2\right) \tag{11}$$

ε is the polanyi potential that is given as:

$$\epsilon = RT\ln\left(1 + \frac{1}{C_e}\right) \tag{12}$$

where R is the universal gas constant (kJ mol^{-1}) and T is the absolute temperature (K). β is related to the mean adsorption energy by the following expression:

$$E = \frac{1}{\sqrt{2\beta}} \tag{13}$$

The nonlinear plot of D-R isotherm is given in Fig. 13. The mean adsorption energy (E) in the D-R isotherm can act as a rule to differentiate chemical and physical adsorption [47]. The value of E greater then 8 KJ mol^{-1} indicates chemical ion exchange adsorption process whereas values of E below 8 KJ mol^{-1} were the characteristic of physical adsorption process [48].`The value of E for EB adsorption onto BI is

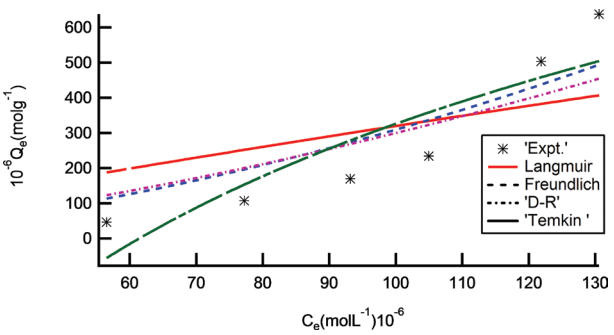

Fig. 13. Nonlinear plots of two parameters adsorption isotherms for adsorption of EB onto BI.

26.13 kJ mol^{-1} indicating that EB adsorption onto BI followed chemical ion exchange adsorption.

The Temkin isotherm assumes that heat of adsorption of all the molecules decrease linearly with the coverage of the molecules due to the adsorbate-adsorbate repulsion and the adsorption of adsorbate is uniformly distributed and that the fall in the heat of adsorption is linear rather than logarithmic [46]. Temkin isotherm is expressed as:

$$q_e = \frac{RT}{b_T}\ln(a_T C_e) \tag{14}$$

where T is the absolute temperature (K) and R is the gas constant (8.31 J mol.K^{-1}) and b_T is related to the heat of adsorption and a_T is the equilibrium binding constant coinciding to the maximum binding energy. The nonlinear plot of Temkin adsorption isotherm model is given in Fig. 13. The values of b_T and a_T were determined and given in Table 3. The Chi- square for Temkin isotherm was small representing that adsorption of EB onto BI followed the Temkin model.

3.3.2. Three parameters adsorption isotherms

The experimental data for the adsorption of EB onto BI was also analyzed using the three parameter isotherm models namely, Hill, Redlich-Peterson and Sips. The three parameter models represent the adsorption capacity as characteristic function of the equilibrium concentration C_e and are empirical in nature [49].

Hill model assumes that adsorption is a cooperative phenomenon, with the ligand binding capability at one site on the macromolecule [50]. The nonlinear form of Hill adsorption isotherm can be expressed as:

$$q_e = \frac{q_H C_e^{n_H}}{k_H + C_e^{n_H}} \tag{15}$$

The plot of Hill model is presented in Fig. 14 and calculated parameters are given in Table 3. The chi-square values of Hill model was small confirming the adsorption of EB onto BI can be defined by Hill model.

Redlich–Peterson is a hybrid isotherm containing both Langmuir and Freundlich isotherms elements which describes equilibrium on homogeneous and heterogeneous surfaces and multilayer adsorption. The Redlich–Peterson (R-P) isotherm [51] contains three parameters, a_{RP}, K_{RP} and g. Non-linear form of R-P isotherm is represented by equation:

$$q_e = \frac{K_{RP} C_e}{1 + a_{RP} C_e^{\,g}} \tag{16}$$

This equation may be used to represent adsorption equilibrium over a wide concentration range of dye molecules. The exponent g lies between 0 and 1. When β = 1, the R-P equation becomes the Langmuir equation, and when β = 0, it becomes the Henry's law [52]. From Fig. 14 it is indicated that experimental data follow R-P model as χ^2 has small values for adsorption of EB onto BI. The calculated R-P model parameters are given in Table 3.

SIPS isotherm is a combined form of Langmuir and Freundlich expressions derived for predicting the heterogeneous adsorption process [53]. Non-linear form of SIPS adsorption isotherm model is represented by:

$$q_e = \frac{K_S C_e^{\,\beta}}{1 + a_S C_e^{\,\beta}} \tag{17}$$

At low adsorbate concentrations, the SIPS isotherm does not obey Henry's law and reduces to the Freundlich isotherm. At high adsorbate concentrations, it follows Langmuir isotherm. The values of SIPS constants were evaluated from Fig. 14 are given in Table 3. The SIPS equation obeys equilibrium data adequately as value of χ^2 was too low (4.69×10^{-9}).

3.3. Adsorption thermodynamics

Thermodynamic parameters indicate the feasibility and spontaneity of adsorption process. The parameters such as change in Gibb's free energy ($\Delta G°$), enthalpy ($\Delta H°$) and entropy ($\Delta S°$) were measured from given equations

$$\ln Kc = \frac{\Delta S°}{R} - \frac{\Delta H°}{RT} \tag{18}$$

$$K_c = \frac{C_a}{C_e} \tag{19}$$

$$\Delta G° = \Delta H° - T\Delta S° \tag{20}$$

where K_c, C_a, C_e, R, and T are the the equilibrium constant, amount of dye (mol L^{-1}) adsorbed onto the adsorbent per litre (L) of the solution at equilibrium, equilibrium concentration (mol L^{-1}) of dye in solution, general gas contant (8.31 J mol.K^{-1}) and absolute temperature (K) respectively. Similarly $\Delta G°$, $\Delta H°$ and $\Delta S°$ are the change in Gibb's free energy (KJ mol^{-1}), enthalpy (KJ mol^{-1}) and entropy (J mol.K^{-1}) respectively. The plots of lnK_c vs. 1/T for adsorption of EB onto BI is represented in Fig. 15. The adsorption change in enthalpy ($\Delta H°$) and entropy ($\Delta S°$) were calculated from slope and intercept of linear Vant Hoff's plot and are given in Table 4. The values of Gibb's free energy ($\Delta G°$) were negative

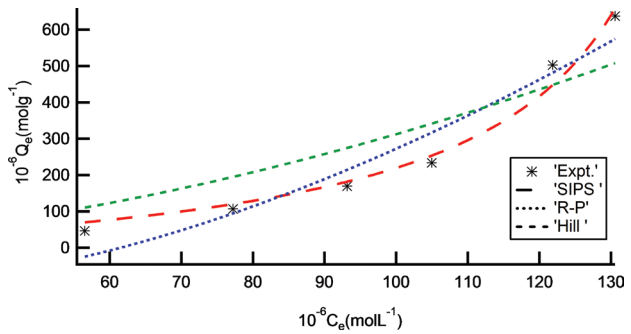

Fig. 14. Nonlinear plots of three parameters adsorption isotherms for adsorption of EB onto BI.

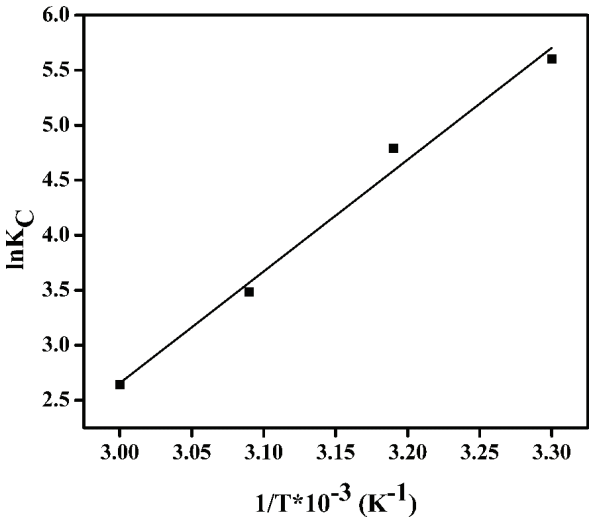

Fig. 15. Plot of $1/T$ vs. $\ln K_c$ for adsorption of EB onto BI.

Table 4
Thermodynamic parameters for adsorption of EB onto BI

ΔH (KJ mol^{-1})	ΔS (J mol^{-1})	ΔG (KJ mol^{-1})			
		303 K	313 K	323 K	333 K
–84.15	231.10	–70.10	–72.41	–74.72	–77.04

at all the temperatures investigated which exhibits the spontaneity and feasibility of adsorption process. The nagative value of enthalpy ($\Delta H°$) shows that adsorption of EB onto BI is an exothermic process. Similarly, the positive value of entropy ($\Delta S°$) denotes the increase in randomnes at the dye-membrane interface during the adsorption of EB onto BI.

4. Conclusions

In this manuscript, the anion exchange membrane (BI) was checked in term of its adsorption potential to remove EB from aqueous solution at room temperature. The percentage removal of EB was enhanced with contact time and amount of adsorbent but decreased with initial dye concentration and temperature. The kinetics study revealed that adsorption of EB onto BI followed the pseudo-second-order kinetic model. The experimental adsorption data was analyzed by two and three parameters nonlinear isotherm models such as Langmuir, Freundlich, Temkin, Dubinin-Radushkevich (D-R), Redlich-Peterson, Hill, Sips and Toth and fitted well to all these isotherms but best followed to Langmuir isotherm model. The negative value of enthalpy ($\Delta H°$) showed that adsorption of EB onto BI is an exothermic process. Hence, this research exhibited that anion exchange membrane (BI) could be employed as an excellent adsorbent for removal of EB from aqueous solution at ambient temperature.

Acknowledgments

The authors are highly thankful to the CAS-TWAS President's fellowship for PhD financial support.

References

[1] R. Khlifi, L. Belbahri, S. Woodward, M. Ellouz, A. Dhouib, S. Sayadi, T. Mechichi, Decolourization and detoxification of textile industry wastewater by the laccase-mediator system, J. Hazard. Mater., 175 (2010) 802–808.
[2] M.T. Yagub, T.K. Sen, S. Afroze, H.M. Ang, Dye and its removal from aqueous solution by adsorption: a review, Adv. Colloid. Interface. Sci., 209 (2014) 172–184.
[3] M.A.M. Salleh, D.K. Mahmoud, W.A.W.A. Karim, A. Idris, Cationic and anionic dye adsorption by agricultural solid wastes: a comprehensive review, Desalination, 280 (2011) 1–13.
[4] A. Srinivasan, T. Viraraghavan, Decolorization of dye wastewaters by biosorbents: a review, J. Environ. Manage., 91 (2010) 1915–1929.
[5] E. Eren, B. Afsin, Investigation of a basic dye adsorption from aqueous solution onto raw and pre-treated sepiolite surfaces, Dyes. Pigm., 73 (2007) 162–167.
[6] P. Janoš, H. Buchtová, M. Rýznarová, Sorption of dyes from aqueous solutions onto fly ash, Water. Res., 37 (2003) 4938–4944.
[7] S. Dawood, T.K. Sen, Removal of anionic dye Congo red from aqueous solution by raw pine and acid-treated pine cone powder as adsorbent: equilibrium, thermodynamic, kinetics, mechanism and process design, Water. Res., 46 (2012) 1933–1946.
[8] Y.C. Sharma, S. Uma, Optimization of parameters for adsorption of methylene blue on a low-cost activated carbon, J. Chem. Eng. Data., 55 (2010) 435–439.
[9] S. Wang, Z.H. Zhu, A. Coomes, F. Haghseresht, G.Q. Lu, The physical and surface chemical characteristics of activated carbons and the adsorption of methylene blue from wastewater, J. Colloid. Interface. Sci., 284 (2005) 440–446.
[10] C.A. Başar, Applicability of the various adsorption models of three dyes adsorption onto activated carbon prepared waste apricot, J. Hazard. Mater., 135 (2006) 232–241.
[11] G. Crini, Non-conventional low-cost adsorbents for dye removal: a review, Bioresour. Technol., 97 (2006) 1061–1085.
[12] Sumanjit, T.P.S. Walia, Use of dairy sludge for the removal of some basic dyes, J. Environ. Eng. Sci., 7 (2008) 433–438.
[13] Q. Sun, L. Yang, The adsorption of basic dyes from aqueous solution on modified peat–resin particle, Water. Res., 37 (2003) 1535–1544.
[14] K.V. Kumar, K. Porkodi, Batch adsorber design for different solution volume/adsorbent mass ratios using the experimental equilibrium data with fixed solution volume/adsorbent mass ratio of malachite green onto orange peel, Dyes. Pigm., 74 (2007) 590–594.
[15] R. Gong, Y. Sun, J. Chen, H. Liu, C. Yang, Effect of chemical modification on dye adsorption capacity of peanut hull, Dyes. Pigm. 67 (2005) 175–181.
[16] N.P. Sumanjit, Adsorption of dyes on rice husk ash, Indian J. Chem. 40 (2001) 388–391.
[17] R.K.M. Sumanjit, S. Rani, T.P.S. Walia, R. Kuar, Adsorptive removal of five acid dyes using various unconventional adsorbents, J. Surf. Sci.Technol., 26 (2010) 77–93.
[18] J.-W. Ma, H. Wang, F.-Y. Wang, Z.-H. Huang, Adsorption of 2,4-dichlorophenol from aqueous solution by a new low-cost adsorbent – activated bamboo charcoal, Sep. Sci. Technol., 45 (2010) 2329–2336.
[19] S. Jain, R.V. Jayaram, Adsorption of phenol and substituted chlorophenols from aqueous solution by activated carbon prepared from jackfruit (artocarpus heterophyllus) peel-kinetics and equilibrium studies, Sep. Sci.Technol., 42 (2007) 2019–2032.
[20] P. Vijayalakshmi, V.S.S. Bala, K.V. Thiruvengadaravi, P. Panneerselvam, M. Palanichamy, S. Sivanesan, Removal of Acid Violet 17 from aqueous solutions by adsorption onto activated carbon prepared from pistachio nut shell, Sep. Sci. Technol., 46 (2010) 155–163.
[21] M.J.Z. Belala, M. Belhachemi, F. Addoun, G. Trouve, Biosorption of copper from aqueous solutions by date stones and palm-trees waste, Environ. Chem. Lett., 9 (2011) 65–69.
[22] Y.-F. Lin, H.-W. Chen, P.-S. Chien, C.-S. Chiou, C.-C. Liu, Application of bifunctional magnetic adsorbent to adsorb metal

cations and anionic dyes in aqueous solution, J. Hazard. Mater., 185 (2011) 1124–1130.
[23] M.U. Dural, L. Cavas, S.K. Papageorgiou, F.K. Katsaros, Methylene blue adsorption on activated carbon prepared from Posidonia oceanica (L.) dead leaves: kinetics and equilibrium studies, Chem. Eng. J., 168 (2011) 77–85.
[24] S. Xiao, M. Shen, R. Guo, Q. Huang, S. Wang, X. Shi, Fabrication of multiwalled carbon nanotube-reinforced electrospun polymer nanofibers containing zero-valent iron nanoparticles for environmental applications, J. Mater. Chem., 20 (2010) 5700–5708.
[25] D. Wesenberg, I. Kyriakides, S.N. Agathos, White-rot fungi and their enzymes for the treatment of industrial dye effluents, Biotechnol. Adv., 22 (2003) 161–187.
[26] J.-S. Wu, C.-H. Liu, K.H. Chu, S.-Y. Suen, Removal of cationic dye methyl violet 2B from water by cation exchange membranes, J. Membr. Sci., 309 (2008) 239–245.
[27] H.-C. Chiu, C.-H. Liu, S.-C. Chen, S.-Y. Suen, Adsorptive removal of anionic dye by inorganic–organic hybrid anion-exchange membranes, J. Membr. Sci., 337 (2009) 282–290.
[28] M.I. Khan, S. Akhtar, S. Zafar, A. Shaheen, M.A. Khan, R. Luque, Removal of Congo Red from aqueous solution by anion exchange membrane (EBTAC): adsorption kinetics and thermodynamics, Materials, 8 (2015) 4147–4161.
[29] M.I. Khan, L. Wu, A.N. Mondal, Z Yao, L Ge, T. Xu, Adsorption of methyl orange from aqueous solution on anion exchange membranes: adsorption kinetics and equilibrium, Membr. Water. Treat., 7 (2016) 23–38.
[30] M.A. Khan, M.I. Khan, S. Zafar, Removal of different anionic dyes from aqueous solution by anion exchange membrane, Membr. Water. Treat., 8 (2017) 259–277.
[31] M.I. Khan, S. Zafar, M.A. Khan, A.R. Buzdar, P. Prapamonthon, Adsorption kinetic, equilibrium and thermodynamic study for the removal of Congo Red from aqueous solution, Desal. Wat. Treat., 98 (2017) 294–305.
[32] M.I. Khan, M.A. Khan, S. Zafar, M.N. Ashiq, M. Athar, A.M. Qureshi, M. Arshad, Kinetic, equilibrium and thermodynamic studies for the adsorption of methyl orange using new anion exchange membrane (BII), Desal. Wat. Treat., 58 (2017) 285–297.
[33] J. Zhang, Q. Zhou, L. Ou, Kinetic, Isotherm, and thermodynamic studies of the adsorption of methyl orange from aqueous solution by chitosan/alumina composite, J. Chem. Eng. Data., 57 (2012) 412–419.
[34] N. Atar, A. Olgun, S. Wang, S. Liu, Adsorption of anionic dyes on boron industry waste in single and binary solutions using batch and fixed-bed systems, J. Chem. Eng. Data., 56 (2011) 508–516.
[35] K.D. Belaid, S. Kacha, M. Kameche, Z. Derriche, Adsorption kinetics of some textile dyes onto granular activated carbon, J. Environ. Chem. Eng., 1 (2013) 496–503.
[36] L. Liu, Y. Lin, Y. Liu, H. Zhu, Q. He, Removal of methylene blue from aqueous solutions by sewage sludge based granular activated carbon: adsorption equilibrium, kinetics, and thermodynamics, J. Chem. Eng. Data., 58 (2013) 2248–2253.
[37] S. Kuo, E.G. Lotse, Kinetics of phosphate adsorption and desorption by hematite and gibbsite1, Soil. Sci., 116 (1973) 400–406.
[38] A. Rahmani-Sani, A. Hosseini-Bandegharaei, S.-H. Hosseini, K. Kharghani, H. Zarei, A. Rastegar, Kinetic, equilibrium and thermodynamic studies on sorption of uranium and thorium from aqueous solutions by a selective impregnated resin containing carminic acid, J. Hazard. Mater., 286 (2015) 152–163.
[39] B. Royer, N.F. Cardoso, E.C. Lima, J.C.P. Vaghetti, N.M. Simon, T. Calvete, R.C. Veses, Applications of Brazilian pine-fruit shell in natural and carbonized forms as adsorbents to removal of methylene blue from aqueous solutions—Kinetic and equilibrium study, J. Hazard. Mater., 164 (2009) 1213–1222.
[40] S. Zakhama, H. Dhaouadi, F. M'Henni, Nonlinear modelisation of heavy metal removal from aqueous solution using Ulva lactuca algae, Bioresour. Technol., 102 (2011) 786–796.
[41] H. Dhaouadi, F. M'Henni, Vat dye sorption onto crude dehydrated sewage sludge, J. Hazard. Mater., 164 (2009) 448–458.
[42] S. Zafar, N. Khalid, M. Daud, M.L. Mirza, Kinetic studies of the adsorption of thorium ions onto rice husk from aqueous media: linear and nonlinear approach, The Nucleus, 52 (2015) 14–19.
[43] M.C. Ncibi, Applicability of some statistical tools to predict optimum adsorption isotherm after linear and non-linear regression analysis, J. Hazard. Mater., 153 (2008) 207–212.
[44] H.M.F. Freundlich, Uber dye adsorption in Losungen, Z. Phys. Chem, (1906) 385–470.
[45] I. Langmuir, The constitution and fundamental properties of solids and liquids, J. Am. Chem. Soc., 38 (1916) 2221–2295.
[46] S. Chen, Q. Yue, B. Gao, Q. Li, X. Xu, Removal of Cr (VI) from aqueous solution using modified corn stalks: characteristic, equilibrium, kinetic and thermodynamic study, Chem. Eng. J., 168 (2011) 909–917.
[47] R. Donat, A. Akdogan, E. Erdem, H. Cetisli, Thermodynamics of Pb^{2+} and Ni^{2+} adsorption onto natural bentonite from aqueous solutions, J. Colloid. Interf. Sci., 286 (2005) 43–52.
[48] B. Hu, H. Luo, H. Chen, T. Dong, Adsorption of chromate and para-nitrochlorobenzene on inorganic–organic montmorillonite, Appl. Clay. Sci., 51 (2011) 198–201.
[49] J.U.K. Oubagaranadin, Z.V.P. Murthy, Isotherm modeling and batch adsorber design for the adsorption of Cu(II) on a clay containing montmorillonite, Appl. Clay. Sci., 50 (2010) 409–413.
[50] K.Y. Foo, B.H. Hameed, Insights into the modeling of adsorption isotherm systems, Chem. Eng. J., 156 (2010) 2–10.
[51] O. Redlich, D.L. Peterson, A useful adsorption isotherm, J. Phys. Chem., 63 (1959) 1024–1026.
[52] M. Brdar, M. Šćiban, A. Takači, T. Došenović, Comparison of two and three parameters adsorption isotherm for Cr(VI) onto Kraft lignin, Chem. Eng. J., 183 (2012) 108–111.
[53] R. Sips, Combined form of Langmuir and Freundlich equations, J. Phy. Chem., 16 (1948) 490–495.